Abstract

Heart ischemia, the precursor to an infarction, is one of the most common diseases in the western world. Today, the electrocardiogram or ECG is the most widely used tool to diagnose the disease. However, it often fails to detect the ischemia or to give an adequate picture of the size and location.

Therefore, the potential of increasing knowledge obtained through mathematical models is very high. In this thesis the bidomain model is used to describe the electrical activity in the heart and body with ischemia incorporated into the model. To solve the equations set up by the bidomain model, the finite element method is used. Different physiological variations have been made to the body, these include changing the location of the heart and varying the conductivities in the body. The solution to the equations is then studied at the body surface. The main question asked is whether it is possible to detect the location and size of different types of ischemia by analyzing the solution.

The methods used for this have been Singular Value Decomposition and Supervised learning. The different vectors obtained from the decomposition are used to distinguish the location and size of the ischemia for different physiological variations.

The results show that it is possible to distinguish the location of the ischemia but that it probably will be more difficult to find the correct size since the change in size is harder to separate from other physiological variations, such as the conductivity of the body.

Although relatively simple methods have been used, they indicate that, with further development, they can be used for the purpose of detecting the different ischemia.

Acknowledgments

I would like to thank my two supervisors, Mats G Larson and August Johansson, for their help with this thesis, always helpful and willing to aid with their knowledge.

Contents

1 Introduction

This thesis was performed at the University of Umeå at the Mathematics Department. The main part of it uses applied mathematics, i.e. application of mathematics and models to describe different areas such as numerical analysis, mathematical physics, mathematical biology and a great deal of what is called computer science. This thesis is about the use of a mathematical model that describes the electrical activity in the heart when ischemia is present. The solution is then studied and analyzed.

1.1 Background

One of the most common diseases in the western world is heart ischemia. Approximately one million people are killed every year [2]. The disease is caused by a lack of blood and oxygen to the heart muscle, which happens when a coronary artery becomes blocked. Ischemia is a precursor of infarction, i.e. if the ischemic condition (lack of blood) persists, the outcome will be an infarction. Traditional ECG readings often fail to detect ischemia [2] and the readings only provide a rather crude picture of the size and location of infarctions. The potential for increasing knowledge and clinical applications using mathematical models are therefore very high.

The use of models to describe physiological properties is growing in popularity. To compute the electrical activity in the heart and the body, models are used to describe how the electrical activity (signals) is generated in the heart and how they distribute throughout the heart and the body. The mathematical model, called the bidomain model, are formulated in terms of differential equations. In order to solve these equations finite element methods are used together with a mesh geometry and an adaptive algorithm which coarsen and refine the mesh where needed. Adaptivity and geometrical modeling are two of the fields studied at the University of Umeå.

This thesis takes advantage of the existing mathematical model and how to solve the equations. Different physiological variations are made to the model and the effects of these variations on the solution (i.e. potential) at the body surface are then studied and analyzed. Certain restrictions are made to the model, for example, it is only the stationary phase of the bidomain model and the ST-segment shift of the ECG that is being studied.

1.2 Purpose

An important question, perhaps *the* question, not only in this thesis but for many who studies the electrical activity in the heart and body is:

Is it possible to detect different types of ischemia based on ECG readings using mathematical models?

As mentioned above, if this question could be answered in a satisfying way, it will lead to increased knowledge about the heart which then could be used in clinical applications.

The overall purpose of this thesis is to study different types of ischemia and, to a greater extent, how the potential (at the torso) is affected when different physiological variations have been made to the model. These are, for example,

the heart location in the body and what happens when the location is changed. Other variations are the conductivities in the lungs, this is done by changing the values at certain discrete steps, but also by creating random conductivities throughout the entire body using the normal distribution. The question then is if it is possible to decide, by analyzing the solution, the location and size of the ischemia.

To analyze the results, the method of Singular Value Decomposition - SVD, and to a lesser extent, Supervised Learning, are used.

The results show that it is possible to separate the four locations for the ischemia. It will probably be more difficult to separate the size of the ischemia from the other perturbations. Although relatively simple concepts used, with further work, they will be able to separate more locations and sizes of the ischemia.

1.3 Disposition of the thesis

The next section is about the physiological background. The functionality of the heart is described and the electrocardiogram (ECG) is explained. What ischemia is and the different types of it used in this thesis are described as well. Section 3 describes the mathematical models used, the so-called bidomain equations. This model describes the electrical activity in the heart and the body with ischemia incorporated into the model. Section 4 contains a summary of the different ways of solving the equations used. The different ways of generating data and the results to these are given in Section 5. Section 6 gives an outline of the specific methods that have been used in order to analyze the solutions to the generated data and the results to these analysis. Also, in this section, a verification of the methods used are made. Four "unknown" ischemia have been generated and these are compared with the knowledge obtained earlier. Finally, the concluding discussion of the obtained results and suggestions on future developments is given Section 7.

2 Physiological Background

In this section a brief explanation of the heart anatomy and the electrocardiogram, or ECG, is given. Also mentioned are the various properties of heart ischemia. The material is taken from [1], [2] and [7]. For more on these subjects, see the aforementioned sources.

2.1 The Human Heart

In the human body, the heart is normally situated slightly to the left of the middle of the thorax, underneath the sternum (breastbone) where it is enclosed by a sac known as the pericardium and is surrounded by the lungs. The mass of the heart is 250-350 g for normal adults. It consists of four chambers, the two upper atria and the two lower ventricles.

Figure 1 shows the anatomy of the heart. The four chambers are seen, separating the right atrium and ventricle from the left atrium and ventricle is a septum. The valves between the atria and the ventricles are shown as well as the largest artery in the body, the aorta, which brings oxygenated blood to all parts of the body.

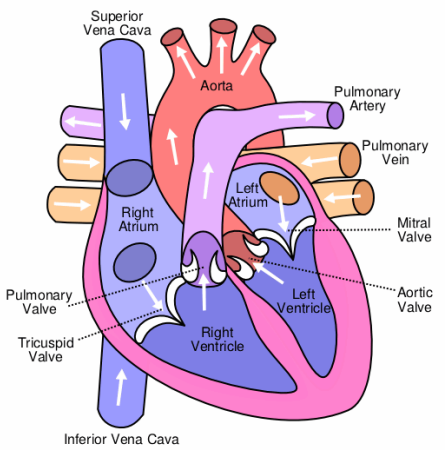

Figure 1: *The human heart.*

The heart wall is made of three distinct layers. The first is the outer epicardium which is composed of a layer of flattened epithelial cells and connective tissue. Beneath this is a much thicker myocardium made up of cardiac muscle. The endocardium is a further layer of flattened epithelial cells and connective tissue which lines the chambers of the heart. The right side of the heart collects deoxygenated blood from the body and pump it into the lungs while the left side of the heart collects oxygenated blood from the lungs and pumps it out to the body. Due to the fact that the left side has to pump blood around the entire body, the left ventricle is much more muscular (1.3 - 1.5 cm thick) than the right (0.3 - 0.5 cm thick). The blood supply to the heart itself is supplied by the left and right coronary arteries, which branch off from the aorta.

2.1.1 The Cardiac Cycle

The function of the heart is to pump blood around the body. Every single beat of the heart involves a sequence of events known as the cardiac cycle, which

consists of three major stages: atrial systole, ventricular systole and complete cardiac diastole. The first stage consists of the contraction of the atria and the corresponding influx of blood into the ventricles. When the blood has left the atria, the atrioventricular valves close. Thereafter the ventricles contracts and the blood flows into the circulatory system. Again, valves closes once the blood has left the ventricles. The third and last phase involves relaxation of the atria and ventricles preparing for refilling of circulatory blood.

2.1.2 Signal Conduction

Electrical impulses from the heart muscle (the myocardium) cause the heart to beat (contract). This electrical signal begins in the sinoatrial (SA) node, located at the top of the right atrium, see Figure 1. The SA node is sometimes called the heart's "natural pacemaker". When an electrical impulse is released from this natural pacemaker, it causes the atria to contract. The signal then passes through the atrioventricular (AV) node. The AV node checks the signal and sends it through the muscle fibers of the ventricles, causing them to contract. The SA node sends electrical impulses at a certain rate, but the heart rate may still change depending on physical demands, stress, or hormonal factors.

2.2 Electrocardiogram - ECG

The electrocardiogram, or ECG, is a graphic recording of the electrical potential differences at the body surface that result from the electrical activity in the heart. The potential differences are caused by sources of electrical current in the active heart muscle. To record the potential difference several leads, 12, are connected to the body. The first ECG measurements was published in 1887 by Augustus D. Waller. Today, it is estimated that one million ECG recordings are performed worldwide on a daily basis, making the ECG the most widely used tool for heart diagnosis. This is due to its simplicity, reliability and the relatively low costs associated with it.

A real ECG taken from a healthy man and a schematic and idealized ECG are shown in Figure 2. The right figure shows how the potential difference recorded by one lead changes during a heart cycle. Typically, three recognizable waves appear with each heartbeat. These are the P wave, the QRS complex and the T wave. Between these waves, there are intervals or segments, e.g. the PQ-interval or the ST-segment. For more information on these waves and the corresponding heart activity, see [1].

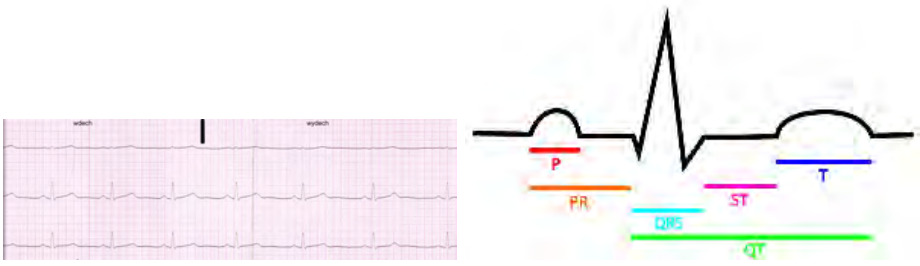

Figure 2: *To the left an electrocardiogram of a healthy man, 21 years old. To the right is an idealized ECG with the different phases.*

Since the ECG is a recording of the electrical activity of the heart, abnormalities in the sinoatrial node or the conduction system will change the ECG. Therefore,

many different pathological conditions may be detected by studying the ECG (more on the different heart conditions can be found in [1]). Of special interest in this thesis is myocardial infarction or ischemic heart disease, see Section 2.3. They can be detected by a characteristic shift in the ST-segment of the ECG, see Figure 2. This shift is caused by lack of blood supply in a portion of the heart. The size and location of the ischemic area will cause the ST-segment to shift up or down compared to the TP-segment.

As mentioned, the ECG is a widely used tool today for heart diagnosis, but there are some weaknesses. Among these are that it could simply fail to detect ischemia [4] and that it only gives a rather crude picture of the size and location of the infarctions [5]. Hence, there is further room for improvement of the technology.

2.3 Ischemia

Ischemia is a restriction in blood supply. Heart ischemia is a disease caused by the lack of blood and oxygen to the heart muscle which happens when a coronary artery, which supplies the heart with blood, becomes blocked. If the ischemic condition persists, the outcome will be an infarction. Therefore, ischemia could be seen as a precursor of infarction.

Depending on the location of the ischemia in the heart wall, it is either classified as subendocardial or transmural. Transmural extends from the endocardium through to the epicardium (classified as full-thickness, or transmural ischemia). The ischemia is also classified as one of the following

- anterior
- posterior
- inferior
- lateral

due to its location. These eight different types of ischemia are illustrated in Figure 3 below.

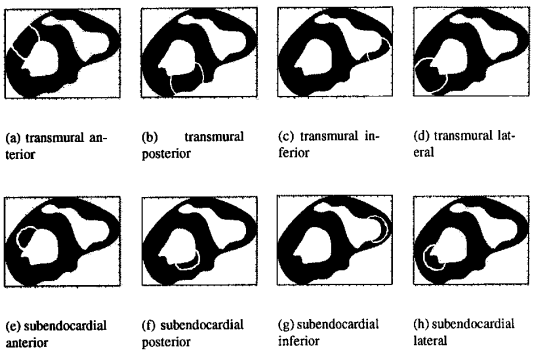

Figure 3: *Eight locations of ischemic regions.*

3 Mathematical Model

The following four sections are taken in large part from the book written by the people at the Simula Research Laboratory [2]. First the body is modeled as a volume conductor, Section 3.1. In Section 3.2 a model for the heart tissue is proposed, which leads to the bidomain model, Section 3.2.2, which was first presented by Tung [6]. Thereafter the heart and the torso is coupled and a short overview of the different models for the ionic current is given in Section 3.3 and then a summary is given for the mathematical model in Section 3.4. A way of incorporating ischemia into the model is presented in Section 3.5 and in the last section the stationary model is presented and the equations that model the stationary ST-phase are given since in this thesis the simulations were performed using only this phase of the ECG.

3.1 Modeling the Body as a Volume Conductor

There are two possible ways to model the human body, the first is to model each cell separately and then couple them together using known coupling mechanisms. However, since the number of cells in the heart and the body is very large, this method would be very difficult and time consuming. Also, the interesting part is the behavior at a larger scale. Therefore, it is better to look at many cells as a continuous volume which leads to a continuous description of the tissue. The chosen volume should be larger than the volume of a single cell but small compared to the problem under study.

3.1.1 A Volume Conductor Model

The averaging process mentioned above allows the modeling of the body as a volume conductor. Starting from Maxwell's equations and assuming quasi-static fields, the electric field E can be written as the gradient of a scalar valued potential u, giving

$$E = -\nabla u \tag{3.1}$$

where the negative sign is convention.[1]

The relation between the current J in a conductor and the conductivity M of the medium is given by $J = ME$. Using equation (3.1) and the relation for the current gives

$$J = -M\nabla u \tag{3.2}$$

Assuming that the net current leaving the volume is zero and denoting the surface of V by S gives

$$\int_S n \cdot J \; dS = 0 \tag{3.3}$$

where n is the outward surface normal of S. The divergence theorem then gives

[1] All quantities in this section must be viewed as averages over a small multicellular volume.

$$-\int_V \nabla \cdot J \; dV = 0 \tag{3.4}$$

This holds for all volumes V, implying that the integrand itself must be zero throughout the domain. Inserting equation (3.2) yields

$$\nabla \cdot (M \nabla u) = 0 \tag{3.5}$$

which is the relation describing the electric potential in a volume conductor with no current sources. Since the heart does generate such sources the equation has to be modified. A common approach is to model the current sources as dipoles, which give rise to a source term on the right hand side of equation (3.5) and the resulting equation is valid throughout the body. Assuming that the body is surrounded by air (an insulating medium), the normal component of the current must be zero on the surface of the body,

$$n \cdot J = 0 \tag{3.6}$$

where n is the outward unit normal on the surface of the body. Using equation (3.2) gives

$$n \cdot M \nabla u = 0 \tag{3.7}$$

The electrical activity in the body is now given by the following two equations

$$\nabla \cdot (M \nabla u) = f, \quad x \in \Omega \tag{3.8}$$
$$n \cdot M \nabla u = 0, \quad x \in \partial\Omega \tag{3.9}$$

where Ω is the body including the heart, $\partial\Omega$ is the surface of the body and f is a given source term. If the boundary value is to have a solution the source term has to satisfy

$$\int_\Omega f \; dx = 0 \tag{3.10}$$

The conductivity value M will vary throughout the body, since different types of tissue have different types of conductivity. These values are given in section 5.1.

Instead of computing the potential distribution in the body, equation (3.5) could be used only in areas immediately surrounding the heart. Since this area (domain) is viewed as a passive conductor, the source term on the right hand side is not necessary. This domain is denoted T and the conductivity and potential by M_T and u_T respectively. The surface of the body is then denoted by ∂T. This domain does not include the heart, therefore an inner boundary also exists[2], this

[2]The inner boundary is between the heart and the surrounding body.

part is denoted by ∂H. As before, the boundary conditions for the body holds (assuming surrounding air). For the inner boundary, it is natural to assume that the potential distribution is known. This gives the following equations

$$-\nabla \cdot (M_T \nabla u_T) = 0, \quad x \in T \tag{3.11}$$

$$n \cdot M_T \nabla u_T = 0, \quad x \in \partial T \tag{3.12}$$

$$u_T = u_{\partial H}, \quad x \in \partial H \tag{3.13}$$

where $u_{\partial H}$ is the known potential distribution on the surface of the heart.

Equations (3.11)-(3.13) can be solved to compute the potential distribution in the surrounding body. Of particular interest, of course, is the surface of the body since that is where the ECG measurements are performed.

3.2 A Model for the Heart Tissue

3.2.1 Excitable Tissue

The heart muscle cells have the ability to pass the electrical signal on to neighboring cells. This enables the electric signal to propagate through the entire heart. This signal propagation takes the form of a so-called depolarization of the cells. When the cells are at rest, a potential difference exists across the cell membrane. The inside potential is called the intracellular potential u_i and this potential is negative compared to the potential between the cells, the so-called extracellular potential u_e.

The potential difference needs to be described using a mathematical model. As previously mentioned, it would be very difficult to model each cell as a separate unit. Therefore, as discussed above, the continuous approach of the tissue is taken, but it must be able to distinguish between the intracellular and extracellular domains.

3.2.2 The Bidomain Model

To be able to include the effects of the potential differences, the heart tissue has to be divided into two separate domains: intracellular and extracellular. Both domains are assumed to be continuous and together they make up the entire heart muscle. The justification for this is due to gap junctions which forms direct contact between the internal of two neighboring cells. In each of the two domains, an electric potential is defined, a quantity averaged over small volumes. This means that every point in the heart muscle have both an intracellular and an extracellular potential.

The two domains are separated by the cell membrane. The same assumptions made for the two domains must also hold for the cell membrane, i.e. continuous and filling the entire heart muscle. The cell membrane acts as an insulator between the domains, yielding the potential difference. However, it allows ions to pass between the membrane via special channels, resulting in an electrical current across the membrane. The potential difference across the membrane is called the transmembrane potential v. It is defined as the difference between the extra- and intracellular potential for every point in the heart.

The quasi-static condition also applies for the heart tissue. Hence the currents in the two domains are given by

$$J_i = -M_i \nabla u_i \tag{3.14}$$
$$J_e = -M_e \nabla u_e \tag{3.15}$$

where J_i is the intracellular and J_e is the extracellular current, M_i and M_e are the conductivities and u_i and u_e are the respective potentials. In Section 3.1.1 it was assumed that there was no build-up of charge at any point. In the bidomain model the cell membrane acts as an insulator and has the ability to separate charge. Therefore, there may be some accumulation of charge in each domain. However, because of the small thickness of the membrane, any accumulation of charge on one side of the membrane immediately attracts an opposite charge on the other side of the membrane. This balance implies that the total charge accumulation in any point is zero, i.e.

$$\frac{\partial}{\partial t}(q_i + q_e) = 0 \tag{3.16}$$

where q_i and q_e is intra- respective extracellular charge. In each domain, the net current into a point must be equal to the sum of the rate of charge accumulation at that point and the ionic current exiting the domain at that point, that is

$$-\nabla \cdot J_i = \frac{\partial q_i}{\partial t} + \chi I_{ion} \tag{3.17}$$
$$-\nabla \cdot J_e = \frac{\partial q_e}{\partial t} + \chi I_{ion} \tag{3.18}$$

where I_{ion} is the ionic current across the membrane. The constant χ represents the area of cell membrane per unit volume. The positive direction of the ionic current is defined to be from the intracellular to the extracellular domain. Combining equations (3.16), (3.17) and (3.18) gives

$$\nabla \cdot J_i + \nabla \cdot J_e = 0 \tag{3.19}$$

or equivalently, using equations (3.14) and (3.15)

$$\nabla \cdot (M_i \nabla u_i) + \nabla \cdot (M_e \nabla u_e) = 0 \tag{3.20}$$

which states that the total current is conserved. The cell membrane is able to separate a certain amount of charge. The amount of charge depends on the transmembrane potential and the capacitive properties of the membrane. The transmembrane potential v is related to the amount of separated charge by the following relation

$$v = \frac{q}{\chi C_m} \tag{3.21}$$

where C_m is the capacitance of the cell membrane and

$$q = \frac{1}{2}(q_i - q_e) \tag{3.22}$$

Combining equations (3.21) and (3.22) and taking the time derivative yields

$$\chi C_m \frac{\partial v}{\partial t} = \frac{1}{2}\frac{\partial (q_i - q_e)}{\partial t} \tag{3.23}$$

and using equation (3.16) gives

$$\frac{\partial q_i}{\partial t} = -\frac{\partial q_e}{\partial t} = \chi C_m \frac{\partial v}{\partial t}. \tag{3.24}$$

Inserting this into equation (3.17) and using equation (3.14) gives

$$\nabla \cdot (M_i \nabla u_i) = \chi C_m \frac{\partial v}{\partial t} + \chi I_{ion} \tag{3.25}$$

Equations (3.20) and (3.25) describe the variations in the three potentials u_i, u_e and v. To eliminate the intracellular potential, the definition of v is used. Since $u_i = u_e + v$, this gives

$$\nabla \cdot (M_i \nabla v) + \nabla \cdot (M_i \nabla u_e) = \chi C_m \frac{\partial v}{\partial t} + \chi I_{ion} \tag{3.26}$$

$$\nabla \cdot (M_i \nabla v) + \nabla \cdot ((M_i + M_e) \nabla u_e) = 0 \tag{3.27}$$

This is the standard formulation of the bidomain model, which was introduced by Tung [6] in the late 70s.

To be able to solve equations (3.26) and (3.27), boundary conditions for u_e and v are needed. If it is assumed that the heart is surrounded by a non-conductive medium, the following holds

$$n \cdot J_i = 0 \tag{3.28}$$

$$n \cdot J_e = 0 \tag{3.29}$$

where n is the outward unit normal vector of the boundary of the heart. Using the expressions for the two currents, and eliminating u_i, gives

$$n \cdot (M_i \nabla v + M_i \nabla u_e) = 0 \tag{3.30}$$

$$n \cdot (M_e \nabla u_e) = 0 \tag{3.31}$$

The ionic current term I_{ion} in equation (3.26) is assumed to be a function of only the transmembrane potential, i.e.

$$I_{ion} = f(v) \tag{3.32}$$

There are many different ways of modeling this term and some of them are mentioned in section 3.3. Now, equations (3.26) and (3.27) together with the boundary conditions given by equations (3.30) and (3.31) and the ionic current term in equation (3.32) form a complete system which can be solved for the potentials u_e and v.

3.2.3 Coupling the Heart and the Body

In Section 3.2.2 it was assumed that the heart was surrounded by a non-conductive medium. But, of course, this is not really the case, since the heart is surrounded by a body which was previously modeled as a passive volume conductor. The electrical potential in the body is given by equation (3.11) and (3.12). However, the boundary condition given by equation (3.13) will have to be modified because the equation must be coupled with the bidomain equations (3.26) and (3.27). Since the heart is surrounded by a conductor, the normal component of the total current must be continuous across the boundary of the heart. Another way of stating this is that on the boundary, the normal component of the current in the heart must be equal to the normal component of the surrounding tissue. The total current in the heart is the sum of the intracellular and extracellular currents. This yields

$$n \cdot (J_i + J_e) = n \cdot J_T \tag{3.33}$$

where n is the outward unit normal of the surface of the heart. Using the expressions for J_i, J_e and J_T, and writing the currents in terms of the main variables u_e, v and u_T and inserting all this in equation (3.33) gives

$$n \cdot (M_e \nabla v + (M_i + M_e)\nabla u_e) = n \cdot (M_T \nabla u_T) \tag{3.34}$$

In order to close the equation system (3.26)-(3.27), additional assumptions have to be made on the coupling between the heart and the surrounding tissue. The boundary conditions given here was originally proposed by Tung [6]. They say that the extracellular domain is in contact with the surrounding tissue while the intracellular domain is completely insulated from the surrounding tissue. The first condition implies that the extracellular potential must be equal to the surrounding potential:

$$u_e = u_T \tag{3.35}$$

The second assumption implies that the normal component of the intracellular potential must be zero on the heart surface giving

$$n \cdot J_i = 0 \tag{3.36}$$

and writing these in the forms of u_e and v gives

$$n \cdot (M_i \nabla v + M_i \nabla u_e) = 0 \tag{3.37}$$

on the heart surface. Inserting this into equation (3.34) gives

$$n \cdot (M_e \nabla u_e) = n \cdot (M_T \nabla u_T) \tag{3.38}$$

The three boundary conditions (3.35), (3.37) and (3.38) couple the equation system (3.26)-(3.27) to (3.11) and (3.12). Combined with an expression of the form given in equation (3.32) for the ionic current term, these equations form a complete system that may be solved for the unknown potentials u_e, v and u_T.

3.3 Models for the Ionic Current

There are several different models for the ionic current. They are commonly grouped into three categories.

- Phenomenological models which reproduce the macroscopically observed behavior of cells.
- The first generation models which try to describe both the observed behavior and the underlying physiology.
- The so-called second generation models which gives a very detailed description of the physiology of the cells.

More about these different kinds of models can be found in [2].

3.4 Summary of the Mathematical Model

The previous sections presented a mathematical model for the electrical activity in the heart and the surrounding body. The surrounding body is modeled as a passive conductor while the heart model was based on viewing the heart as two continuous domains, the intra- and extracellular. The complete model is given by

$$\frac{\partial s}{\partial t} = F(s, v, t) \qquad x \in H \tag{3.39}$$

$$\nabla \cdot (M_i^* \nabla v) + \nabla \cdot (M_i^* \nabla u_e) = \frac{\partial v}{\partial t} + I_{ion}^* \qquad x \in H \tag{3.40}$$

$$\nabla \cdot (M_i^* \nabla v) + \nabla \cdot ((M_i^* + M_e^*) \nabla u_e) = 0 \qquad x \in H \tag{3.41}$$

$$\nabla \cdot (M_T^* \nabla u_T) = 0 \qquad x \in T \tag{3.42}$$

$$u_e = u_T, \qquad x \in \partial H \tag{3.43}$$

$$n \cdot (M_i^* \nabla v + (M_i^* + M_e^*) \nabla u_e) = n \cdot (M_T^* \nabla u_T) \qquad x \in \partial H \tag{3.44}$$

$$n \cdot (M_i^* \nabla v + M_i^* \nabla u_e) = 0 \qquad x \in \partial H \tag{3.45}$$

$$n \cdot (M_T^* \nabla u_T) = 0 \qquad x \in \partial T \tag{3.46}$$

Equation (3.39) is a system of ordinary differential equations that describe the electro physiological behavior of the heart cells. The following two equations,

(3.40) and (3.41) describes the signal propagation in the heart tissue. Equation (3.42) describes the potential distribution in the surrounding body. The connection between the heart and the body is given by the boundary conditions (3.43)-(3.45) and finally, equation (3.46) gives the boundary condition on the body surface.

Note that the system (3.39)-(3.46) has been scaled with the membrane capacitance C_m and the surface to volume ratio χ. The resulting scaled quantities are given by

$$M_i^* = \frac{1}{C_m \chi} M_i \qquad M_e^* = \frac{1}{C_m \chi} M_e \tag{3.47}$$

$$M_T^* = \frac{1}{C_m \chi} M_T \qquad I_{ion}^* = \frac{1}{C_m \chi} I_{ion} \tag{3.48}$$

3.5 Incorporating Ischemia

According to biological observations [2], the cells in an infarcted region in the heart are not excitable. Therefore, the tissue in such a zone behaves like a passive conductor, which means that an ischemia can be incorporated into the model by removing the ion transport in the infarcted area. Another way of saying this is that the conductivities in healthy and ischemic cells are different with the ischemic tissue having a lower conductivity. The transmembrane potential v is another parameter that differs between the two regions.

To simulate these two regions, a smooth and narrow transition is introduced between the healthy and the ischemic tissue, which is also in accordance with the physiological situation. The ischemic region is denoted by D and is introduced by the level set function

$$\phi(x) = \begin{cases} < 0 & x \in D \\ > 0 & x \in H \backslash D \end{cases} \tag{3.49}$$

The notation G is used for the Heaviside function. G_τ is the smooth approximation of $G(x)$

$$G_\tau(x) = \frac{1}{2} + \frac{1}{\pi} \arctan\left(\frac{x}{\tau}\right) \tag{3.50}$$

Now, using the smooth Heaviside function, the transmembrane potential v can be written as

$$v(\phi) = a_1[1 - G_\tau(\phi)] + a_2 G_\tau(\phi) \tag{3.51}$$

where the parameter labeled a_1 is for the ischemic tissue and a_2 is the parameter for the healthy tissue.

The conductivities for the intracellular and extracellular conductivities, M_i and M_e, are now changed. The intracellular conductivity is formulated as

$$K_i(x) = \begin{cases} S_i(x) & x \in D \\ M_i(x) & x \in H \backslash D \end{cases} \tag{3.52}$$

and the extracellular conductivity K_e is given analogously.

The Heaviside function is once again utilized, meaning that the conductivities are given by

$$K_i(\phi) = S_i[1 - G_\alpha(\phi)] + M_i G_\alpha(\phi) \tag{3.53}$$

and, again, analogously for K_e.

The changed subscript for the smooth Heaviside function means that a different smoothing may be used for the conductivities.

3.6 Stationary Model

In this thesis, the bidomain model is restricted to a stationary model, or more precisely, the stationary ST-phase of the ECG (see Figure 4). It is the second equation of the bidomain model as expressed in equations (3.40) and (3.41) that is the interesting part for the stationary model. Note that the extracellular potential u_e is the (unknown) variable.

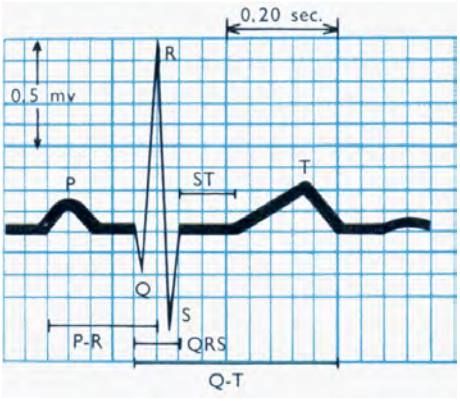

Figure 4: *The electrocardiogram with the different phases. Note the ST-phase.*

To summarize, the complete stationary mathematical model for the ST shift segment is as follows[3]

$$\nabla \cdot ((K_i + K_e)\nabla u_e) = -\nabla \cdot (K_i \nabla v) \qquad x \in H \tag{3.54}$$

$$\nabla \cdot (M_T \nabla u_T) = 0 \qquad x \in T \tag{3.55}$$

$$u_e = u_T \qquad x \in \partial H \tag{3.56}$$

$$n_H \cdot (K_e \nabla u_e) = -n_T \cdot (M_T \nabla u_T) \qquad x \in \partial H \tag{3.57}$$

$$n_H \cdot (K_i \nabla (v + u_e)) = 0 \qquad x \in \partial H \tag{3.58}$$

$$n_T \cdot (M_T \nabla u_T) = 0 \qquad x \in \partial T \tag{3.59}$$

[3]To indicate that the ischemia has been incorporated, the indices introduced in section 3.5 are now used, i.e. K instead of M inside the heart.

The above equations are the governing equations during the ST-phase with ischemia incorporated. These are the equations used when the simulations are performed.

4 Computational Methods

PhD students Johansson and Bengzon at Umeå University have developed code that implements the adaptivity and geometry in the stationary model. In the following sections the ways of solving these equations and how to implement them in a 3-dimensional case are briefly described. The first section describes the FEM technique. Section 4.2 describes the mesh that has been used for the geometry of the body and the last Section, 4.3, describes the adaptive algorithm.

4.1 The Finite Element Method

To solve the equations given in Section 3.6, the finite element method (FEM) is used. This is a method that is used for finding approximate solution of partial differential equations by projection on a finite-dimensional subspace. To solve the PDEs there are two ways of approaching the problem. One is to eliminate the differential equation completely (steady state problems) and the other is to render the PDE into an equivalent ordinary differential equation, which is typical for time dependent problems.

The stationary Bidomain equations in this thesis can be written in variational form as

$$a(u, v) = l(v), \quad \forall v \in V \tag{4.1}$$

The finite element method is then to find $\tilde{u}_h \in V_h$ such that

$$\tilde{a}(\tilde{u}_h, v) = \tilde{l}(v), \quad \forall v_h \in V_h \tag{4.2}$$

where $V_h \subset V$ is a space of piecewise polynomials (trilinear functions) defined on the triangulation (hexahedra). The $\tilde{}$ quantity is used because the conductivities and the transmembrane potential are approximated on a coarser mesh when they are defined on a fine mesh.

4.2 The Mesh

The aforementioned mesh is based on hexahedra. This mesh is build on a surface triangulation based on true MRI[4] data obtained from Simula Research Laboratory in Oslo. This geometry is shown in Figure 5. As seen in the figure only the lower part of the heart is used. This reduction is standard today in simulations performed around the world. Mainly because it is the difference in the ST-region that is being studied and during this time it is the lower part of the heart that is being (de)polarized. Another reason is that the geometry of the upper part is a lot more complicated.

In order to use the hexahedral mesh, it must be known what sort of tissue each hexaeder represents. An identification process is therefore made to discern the torso, the lungs, the heart tissue and the ventricles. After that, the hexahedral mesh is built, see Figure 6.

The advantage with using a mesh based on hexahedra is that it is easy to construct a mesh from an almost arbitrary geometry and then refine and coarsen

[4]Magnetic Resonance Imaging.

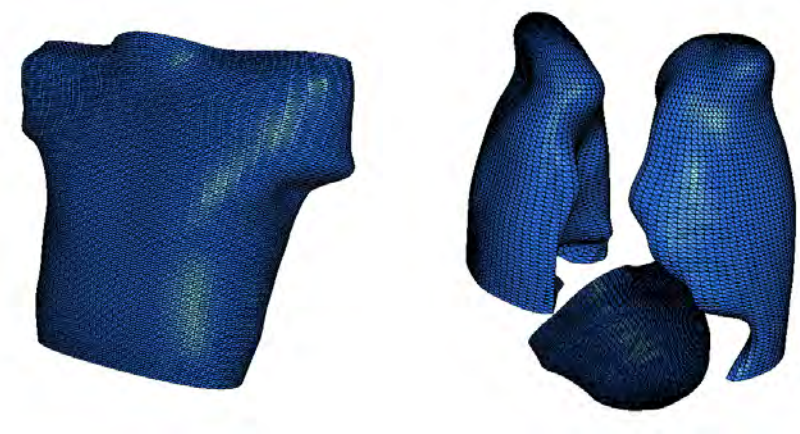

Figure 5: *The geometry of the body. Also shown are the lungs and the heart.*

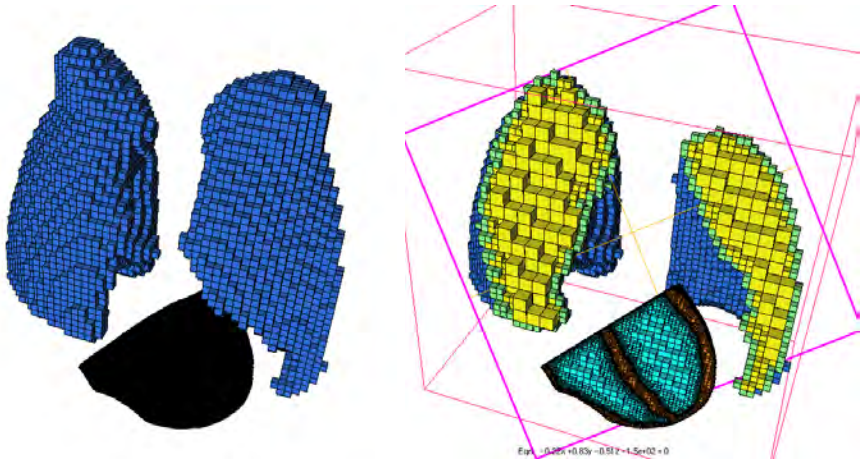

Figure 6: *The different parts of the body in hexahedral form.*

it where needed. It is also possible to handle many different meshes for the same problem. The primal and dual problem (Section 4.3.1) have their own meshes.

The conductivities and the load are specified on the fine mesh. When this has been done, the mesh is coarsened. Information is propagated by interpolation, but the original data is not abandoned. It is possible to coarse the ischemic region differently than the other regions[5].

4.3 Adaptivity

When the simulations are performed, they should produce results that are globally accurate. However, due to the fact that ECG plays a crucial role when measuring the activity of the heart, i.e. the potentials are measured on the surface of the torso, certain areas are more interesting then others. Therefore, it is important that the measurements at these regions are correct. Hence, the error in the measurement points on the torso should influence the computation.

[5]In this thesis, the mesh is more refined in the ischemic region.

4.3.1 The Dual Problem

Let $m(u)$ be the (linear) function of interest (i.e. the potential on the torso). Then $m(u) - m(\tilde{u}_h)$ is the error of interest. To find an expression of the error, the dual problem is as follows

$$m(v) = \tilde{a}(v, \phi), \forall v \in V \tag{4.3}$$

where m could be large in a region w close to the measurement points, for example

$$m(v) = \int_w v\psi \, dx \tag{4.4}$$

where ψ is a smoothed delta function.

In the program, the region for the dual problem was chosen as shown in Figure 7.

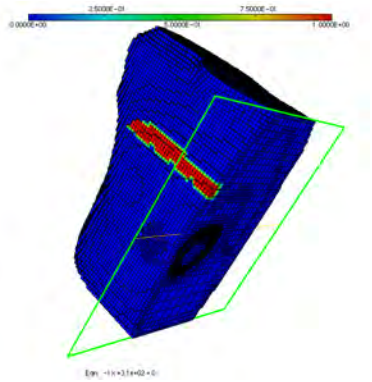

Figure 7: *The dual problem. The band on the torso (where the weight of the dual problem has been implemented, ψ) that has been selected is clearly seen.*

The results from the simulations will, inevitably, have a numerical error. There are three parts that will contribute to this error and these are

- FEM discretization error.
- Error in the conductivities $M - \tilde{M}$.
- Error in the location of the infarction $f - \tilde{f}$.

The last two include modeling errors and data errors due to the fact that a coarser mesh has been used in the simulations. The dual problem is then given by

$$\begin{aligned} m(u) - m(\tilde{u}_h) &= m(e) = \tilde{a}(e, \phi) \\ &= \tilde{a}(e, \phi - \pi\phi) \\ &= \tilde{l}(\phi - \pi\phi) - \tilde{a}(\tilde{u}_h, \phi - \pi\phi) \\ &+ \tilde{a}(u), \phi) - a(u, \phi) \\ &+ l(\phi) - \tilde{l}(\phi) \\ &= I + II + III \end{aligned} \tag{4.5}$$

The first part, the FEM discretization error, can be estimated by

$$\begin{aligned} I &= \tilde{l}(\phi - \pi\phi) - \tilde{a}(\tilde{u}_h, \phi - \pi\phi) \\ &= (\tilde{R}(\tilde{u}_h), \phi - \pi\phi) \\ &= \sum_K (r_K(\tilde{u}_h), \phi - \pi\phi) \end{aligned} \tag{4.6}$$

i.e. element-wise residual contributions. On an element K the following yields

$$|(r_K(\tilde{u}_h), \phi - \pi\phi)| \leq R_K(\tilde{u}_h) \cdot W_K(\phi) \tag{4.7}$$

where

$$R_K(\tilde{u}_h) = \begin{bmatrix} \|f + \nabla \cdot M\nabla\tilde{u}_h\|_K \\ h_k^{-1/2}\|[n \cdot \nabla u]\|_{\partial K}/2 \end{bmatrix} \tag{4.8}$$

and

$$W_K(\phi) = \begin{bmatrix} \|\phi - \pi\phi\|_K \\ h_k^{-1/2}\|\phi - \pi\phi\|_{\partial K} \end{bmatrix} \tag{4.9}$$

There is also two errors in data, but in this thesis only the first part of the error contribution was implemented in the code. However, with them, the total error element indicator may be written

$$\rho_k = R_K(\tilde{u}_h) \cdot W_K(\phi) + \max_K |M - \tilde{M}|\|\nabla\tilde{u}_h\|\nabla\tilde{\phi}_h\| + \|f - \tilde{f}\|\|\tilde{\phi}_h\| \tag{4.10}$$

where the first product corresponds to the FEM discretization error. The total error element indicator will lead to the adaptive algorithm which is summarized in the following two steps

- Find elements with large error indicators ρ_k.
- Refine these to improve the discretization error.

The code generates two solutions, the primal, i.e. the potential, and the dual solution. This thesis only examines the primal solution. The below figure shows the primal solution at the first simulation step to the left and the solution after 15 steps to the right. The figure is a cross-section of the body.

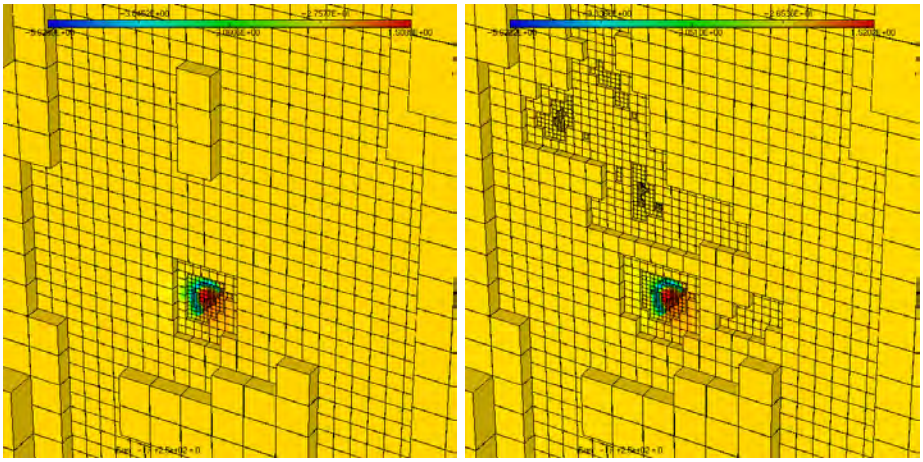

Figure 8: *Primal solution, beginning and after 15 steps.*

The result of the adaptivity is clearly visible in the right figure. The mesh has been refined around the heart region (middle of the figure) and at the region which was chosen for the dual problem, i.e. the torso.

5 Generating Data and Results

The code that has been written and which implements the various techniques mentioned in the previous section has been used to generate solutions. Several additional functions have been written (in the code) that changes the initial conditions in different ways. These are described in the following sections and the obtained solutions, i.e. potential u at a line x on the torso, are shown in the figures.

In figures where all four ischemic regions have been plotted, different colors have been used to symbolize each ischemia. Throughout, when all four ischemias are present in one and the same figure, red is the anterior, green is the posterior, blue is the inferior and yellow is the lateral ischemia. For most of the results below, one particular ischemic region has been used, which is the posterior transmural ischemia. If nothing else is mentioned in the text, this is the ischemia that has been used.

The solution exist in the entire domain. But, during the time this thesis was done, due to the adaptivity, there exists problems around the boundary of the torso. Therefore the solution was taken a few mm inside the torso.

The results from the line on the torso were stored in a matrix where the columns represented the solution for each type of parameter change. Different concepts were used to analyze the results. Those concepts and their subsequent results are described in Section 6.

5.1 Conductivities

The geometry consists of the heart, the lungs and the surrounding body, see Figure 5, with the ischemic region incorporated into the heart. Table 1 shows the different conductivities that have been used in the code. The values are taken from [8] and [9].

Table 1: *The conductivities in the different regions of the body.*

Parameter	Value [mS/cm]
Torso M_T	2.39
Lungs M_T	0.96
Heart ventricles	2.39
M_i	3.0
M_e	2.01
S_i	0.2
S_e	1.0
a_1	40
a_2	90

5.2 Location of the Heart

The heart could be translated in all three directions but when the simulations were performed the translation was restricted to the x-y directions. It was not possible to translate the heart more than a few mm or else it would have been situated outside the body or would have touched the lungs. Additional

code was also written that made it possible to scale the heart but has not been implemented in this thesis. The ischemic region is translated (and scaled) accordingly.

Figure 9 shows the potential on the torso for the posterior ischemia. It has nine different sub figures. These figures have been laid out in a x, y - coordination system where the middle figure is the heart as it is located when no translation has taken place. The heart has been translated in steps of 5 mm. The upper left figure corresponds to the coordinates (-5, 5), i.e. the heart has been translated 5 steps in both directions, and the lower right figure corresponds to (5, -5). Figure 10 shows all translations in the same figure.

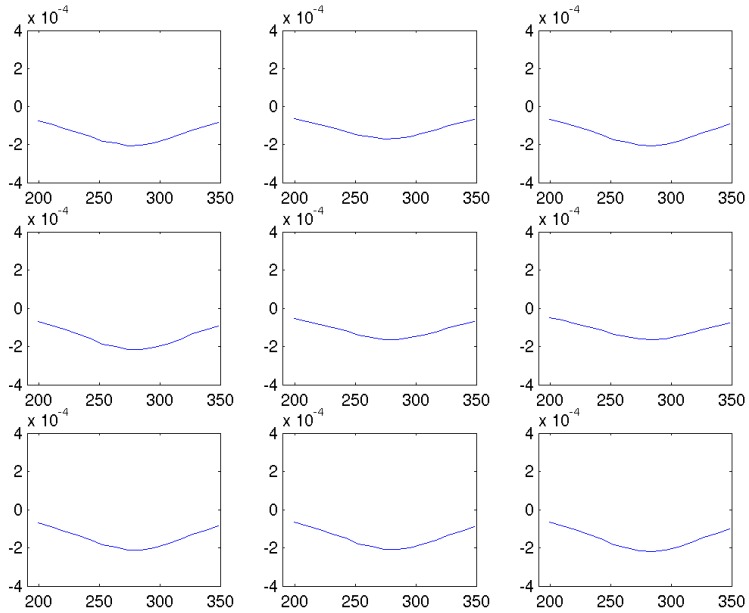

Figure 9: *Heart translation for the posterior ischemia.*

The translation of the heart causes a slight change in the results. Similar results were obtained for the other three ischemic regions. All four ischemic regions and their results are shown in Figure 11 with the normalized results in Figure 12.

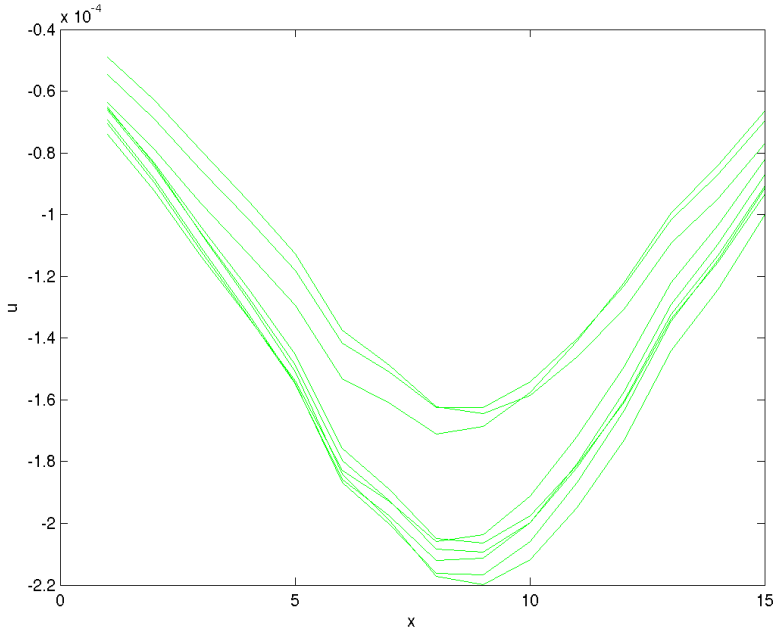

Figure 10: *Heart translation for the posterior ischemia.*

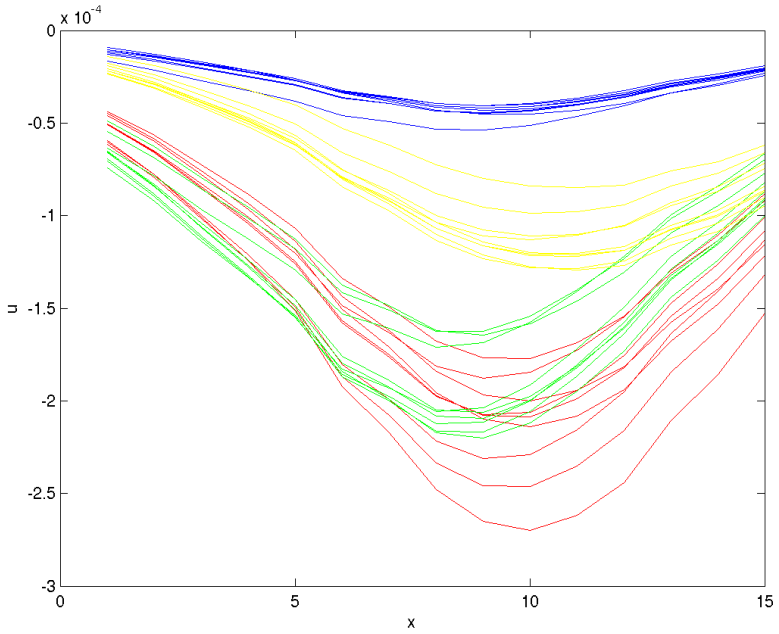

Figure 11: *Heart translation for all four ischemic locations.*

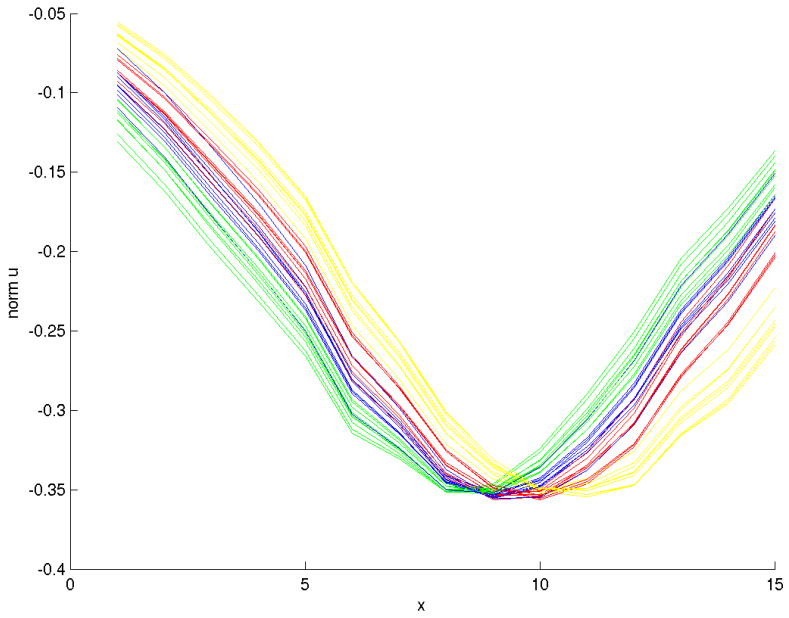

Figure 12: *Heart translation for all four ischemic locations. Normalized results.*

5.3 Location and Size of the Ischemia

As mentioned in Section 2.3 there are four different locations of ischemic regions for the transmural and subendocardial ischemia respectively. To simulate the location and size of the ischemic region it was modeled as a sphere with radius r. For most cases in this thesis the regions were restricted to the transmural ischemia[6], i.e. the radius was sufficiently large to cover the entire heart wall, see Figure 3).

However, the effect on the solution caused by the size of the ischemia was also studied, this was done by altering the radius. This meant that when the radius was smaller, subendocardial ischemia was studied. Figure 13 shows the location of the posterior transmural ischemia in the simulated heart. The different locations were based on Figure 3 (see Section 2.3).

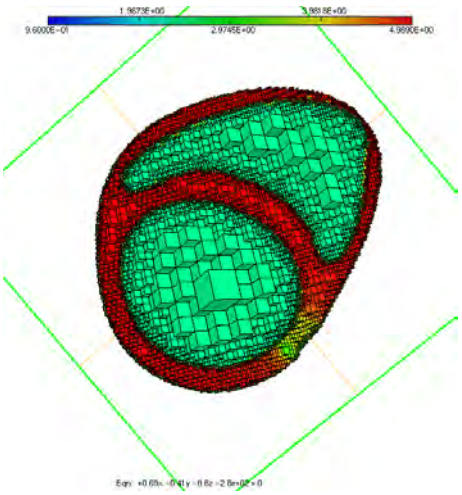

Figure 13: *Location of posterior transmural ischemia in simulated heart. The ischemic region can be seen in the lower right corner of the heart.*

Figure 14 shows the results when the size of the (posterior) ischemic region has been altered (e.g. the radius of the ischemic sphere increases in certain discrete steps, see Section 5.3). The uppermost curve corresponds to the lowest radius and the lowest curve is the one corresponding to the largest radius. In Figure 15, the results have been normalized.

The results from all four ischemic regions are shown in Figure 16 and Figure 17 shows the normalized results.

[6]Where the location of the ischemia extends from the endocardium through to the epicardium.

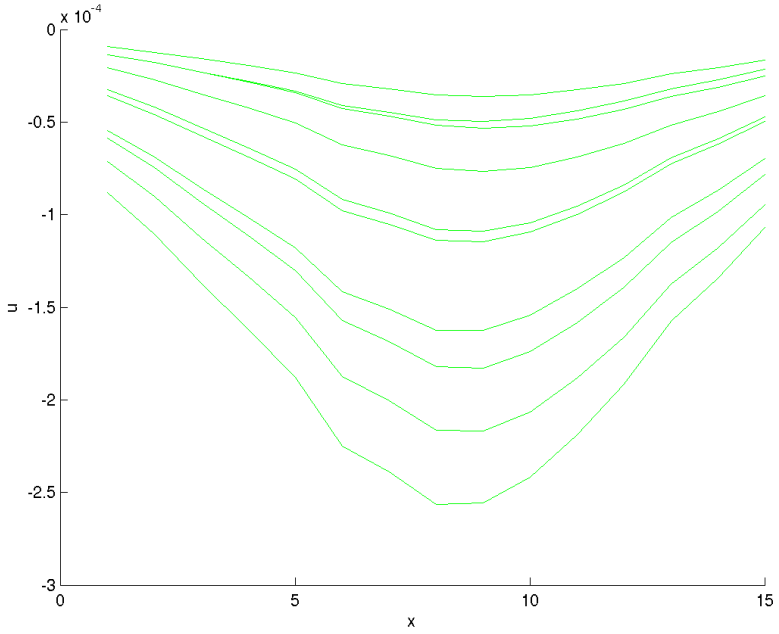

Figure 14: *Varying sizes on the posterior ischemia.*

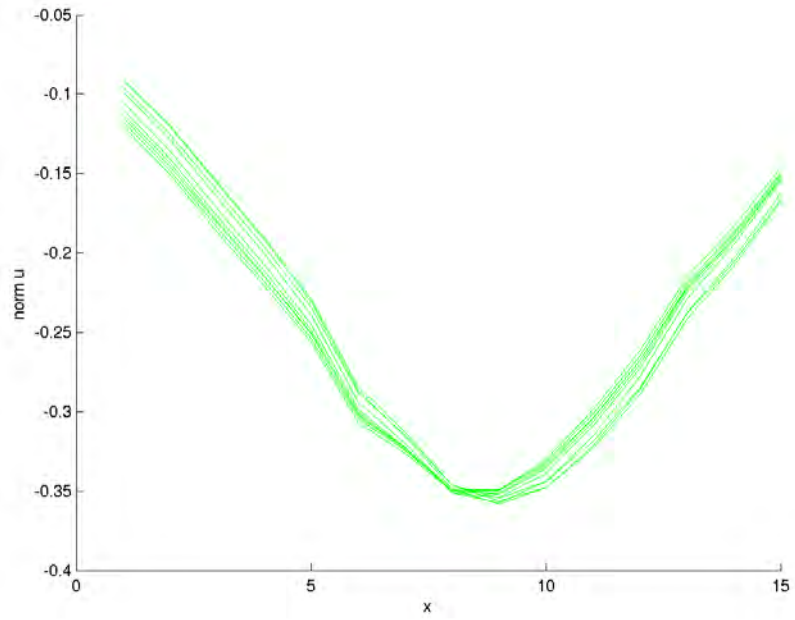

Figure 15: *Normalized results of varying sizes on the posterior ischemia.*

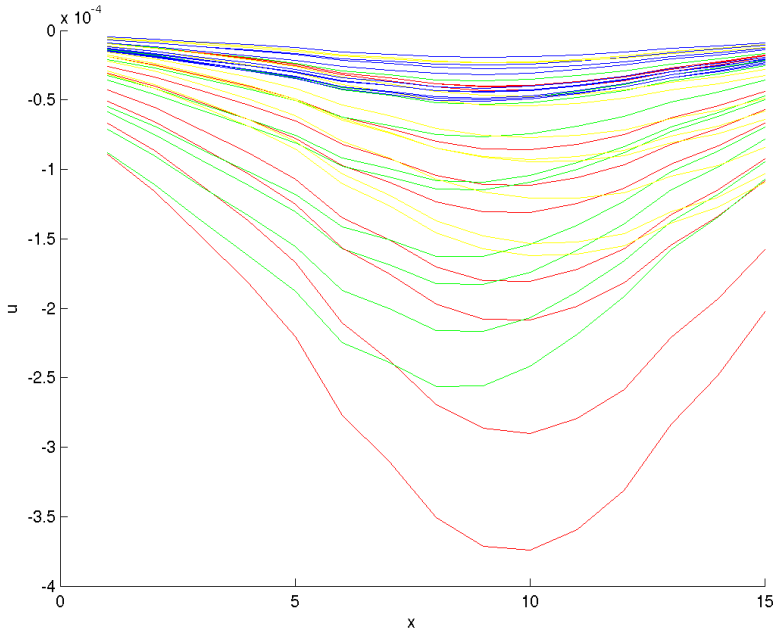

Figure 16: *Varying sizes on the ischemic regions for all four locations.*

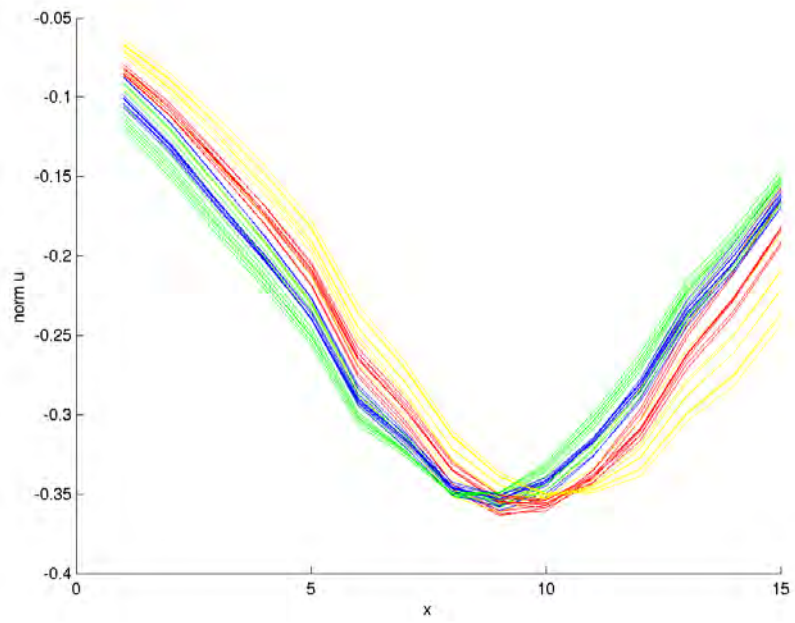

Figure 17: *Normalized results of varying sizes on the ischemic regions for all four locations.*

5.4 Varying Conductivity in the Torso and the Lungs

When simulations were performed for the heart translation the conductivity values for the different parts of the body (e.g. lungs, heart, etc.) had the values described in Section 5.1. In real life it is likely that the conductivities varies, at least a little, and the effect of this when implemented into the model was studied. The conductivity in the different parts of the body was therefore changed in several ways.

5.4.1 Varying Conductivity in the Lungs

First, the effect on the solution caused by different conductivities in the lungs was studied. The conductivity values were changed in certain discrete steps. The conductivity used in the case of the translation of the heart was 0.96 mS/cm. The conductivity value was taken in the region 0.36 - 1.56 mS/cm.

Figure 18 shows the results from the posterior ischemia and the normalized results are shown in Figure 19. The uppermost line corresponds to 0.36 mS/cm and then in increasing order in steps of ten (and five around the original value, 0.96 unit) until the lowest line which corresponds to 1.56 mS/cm. The three middle values 0.91, 0.96 and 1.01 mS/cm have the colors yellow, blue and green respectively.

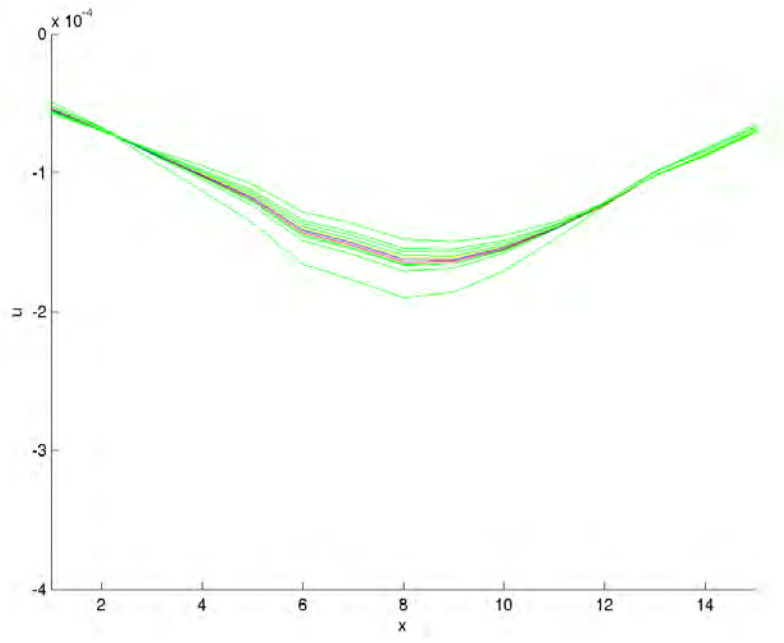

Figure 18: *The conductivities in the lungs have been changed.*

Figure 20 shows the results from all four ischemic regions when the conductivity in the lungs have been changed in discrete steps (as described above) and Figure 21 shows the normalized results.

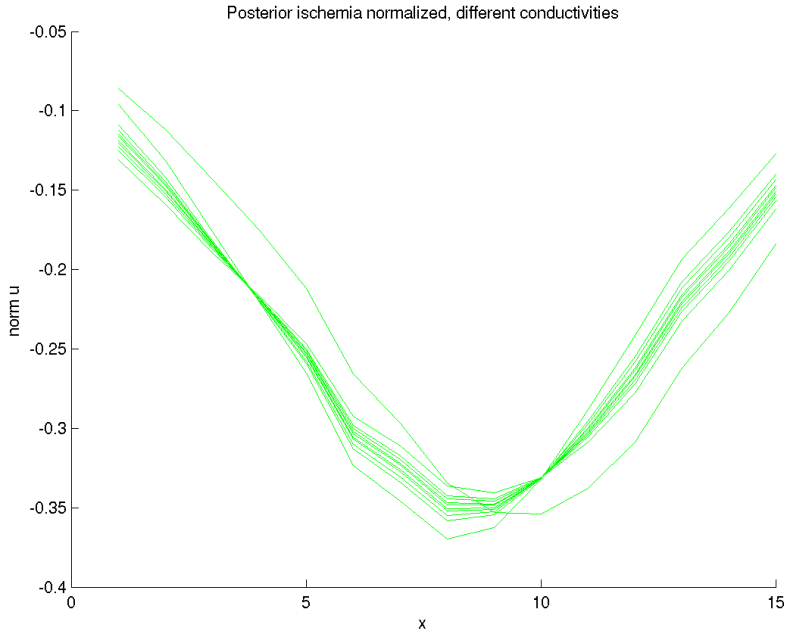

Figure 19: *Normalized results when the conductivities in the lungs have been changed.*

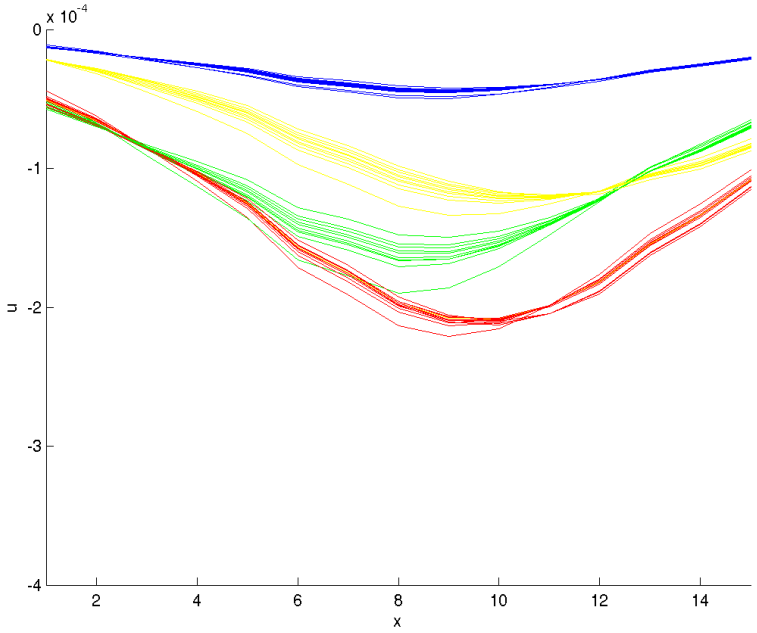

Figure 20: *Results from all four ischemia when the conductivities in the lungs have been changed.*

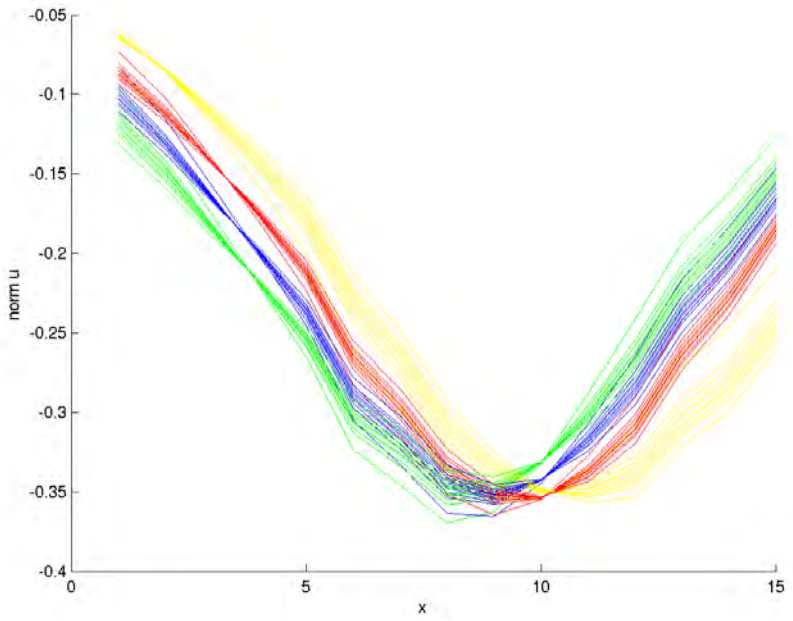

Figure 21: *Normalized results from all four ischemia when the conductivities in the lungs have been changed.*

5.4.2 Stochastic Variations in the Body

The other effect that was studied was when stochastic variations were applied to the body. This was done using the normal distribution. The conductivity values were randomly created using the values described in Section 5.1 as mean values and the standard deviations was set as 5 and 10% of the mean value. The Box-Muller transform [10] was used to generate the normal distribution. Twenty solutions were simulated.

The results using a standard deviation of 5 % of the mean value are shown in Figure 22 with Figure 23 showing the normalized results.

Using a standard deviation of 10 % and performing new simulations, the results are shown in Figure 24 with Figure 25 showing the normalized results.

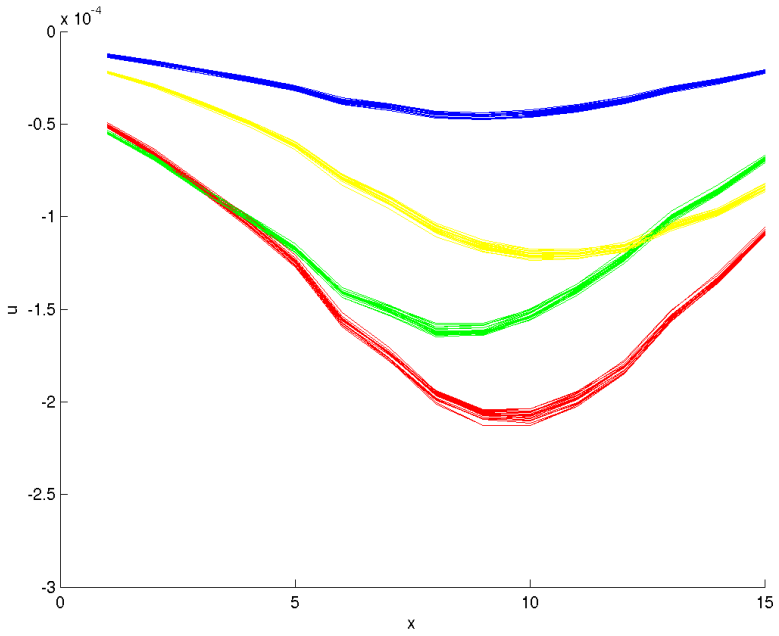

Figure 22: *The conductivities in the body have been varied using normal distribution with a standard deviation of 5 % of the mean value.*

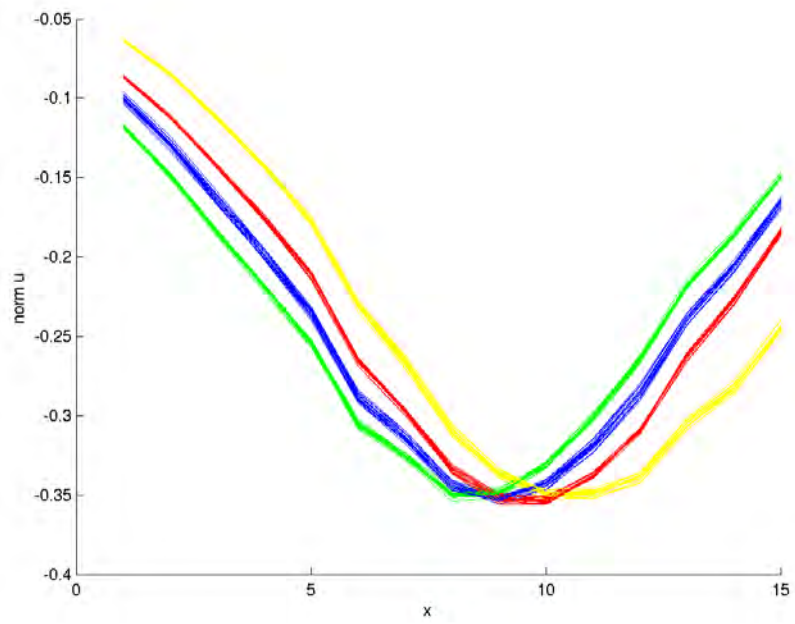

Figure 23: *Normalized results when the conductivities in the body have been varied using normal distribution with a standard deviation of 5 % of the mean value*

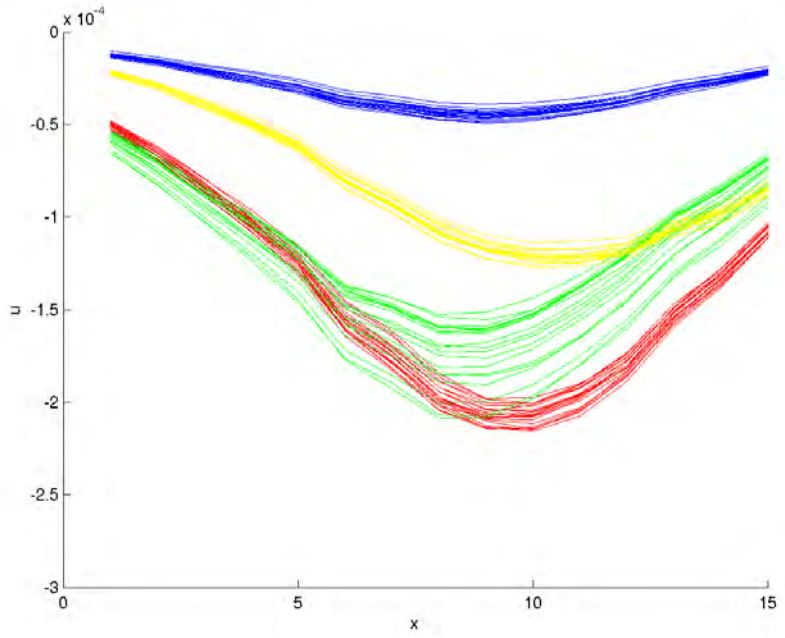

Figure 24: *The conductivities in the body have been varied using normal distribution with a standard deviation of 10 % of the mean value.*

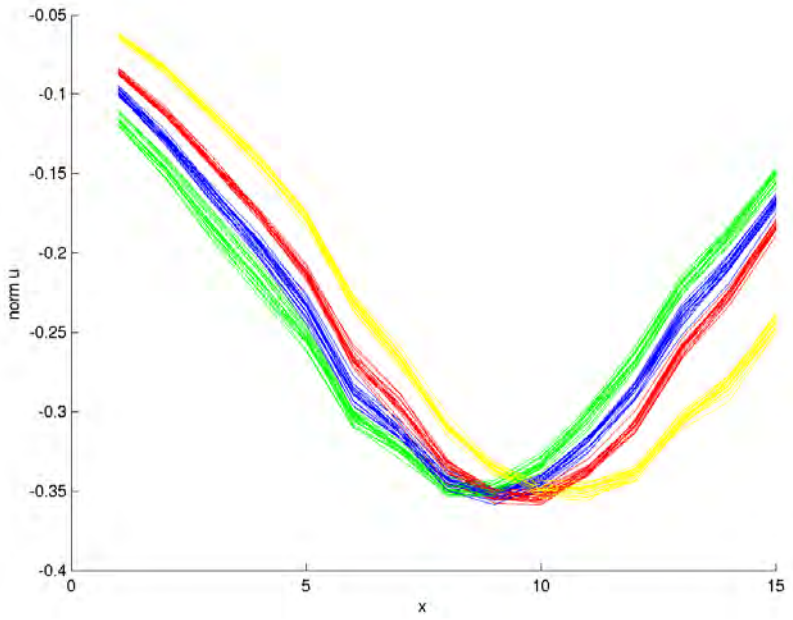

Figure 25: *Normalized results when the conductivities in the body have been varied using normal distribution with a standard deviation of 10 % of the mean value.*

6 Analysis

The main question of this thesis is if it is possible to decide the size and location of the ischemic region based on an examination of the solution at the torso. Different physiological variations have been utilized to generate different solutions. These solutions will be analyzed one by one but the idea is that they will all contribute to an answer to the above question. To analyse the data the Singular Value Decomposition or SVD for short will be used to compute mean values of the measurements. These corresponds to different values of certain physiological variations. The mean values are robust under variations.

To analyze the variation of the computed electrical activities at the torso the Singular Value Decomposition is employed. The SVD is a matrix decomposition which says that every matrix $A \in R^{m\times n}$ can be written as

$$A = U\Sigma V^T \tag{6.1}$$

where $U \in R^{m\times m}$ and $V \in R^{n\times n}$ both are orthogonal matrices. $\Sigma \in R^{m\times n}$ is a matrix on the form

$$D = \begin{pmatrix} D & 0 \\ 0 & 0 \end{pmatrix} \tag{6.2}$$

where $D \in R^{r\times r}$ is a diagonal matrix $D = diag(\sigma_1, \sigma_2, \ldots \sigma_r$ where $r = rank(A)$ and $\sigma_1 \geq \sigma_2 \geq \cdots \geq \sigma_r > 0$. See [3] for a proof of this result.

The SVD is often used to compute approximations of lower rank of the given matrix A. The SVD may be written

$$A = U\Sigma V^T = \sigma_1 u_1 v_1^T + \sigma_2 u_2 v_2^T + \cdots + \sigma_r u_r v_r^T \tag{6.3}$$

and for $1 \leq k \leq r$, A_k is defined as

$$A_k = \sigma_1 u_1 v_1^T + \sigma_2 u_2 v_2^T + \cdots + \sigma_r u_r v_k^T. \tag{6.4}$$

Thus by omitting the smallest singular values a useful approximation can be obtained. It can be shown that the approximation A_k of A using the k largest singular values is the closest matrix of rank k to A in the Frobenius norm[7]. If the singular values are rapidly decaying then the matrix is effectively of lower rank. This approximation is often used in practice to remove noise.

To analyse the dependency of the measurements on variations a matrix is formed where the columns correspond to the measurements for the different perturbations. Next we perform a SVD on this matrix. Then each measurement U can be written as

$$U \approx \delta_0 U_0 + \delta_1 U_1 + \delta_2 U_2 + \ldots \tag{6.5}$$

[7]The Frobenius norm of an $m \times n$ is the Euclidean norm of the matrix considered as a vector in R^{mn}.

Here U_0 corresponds to the mean value of the measurements and the next terms $U_1, U_2, \ldots$ captures the main part of the perturbation caused by the variations. For the analysis, it is important that the studied physiological variations give rise to low dimensional physiological variations.

Assume a number of different locations for the ischemia are studied and a certain physiological variation. For each location i the measurements can be written in the form

$$U^i \approx \delta_0^i U_0^i + \delta_1^i U_1^i + \delta_2^i U_2^i + \ldots \tag{6.6}$$

Now, assume that a measurement U^* has been obtained and that one wants to determine which of the locations of the ischemia is most likely. Then the simplest procedure is to study the scalar products

$$(U^*, U_0^i) \tag{6.7}$$

and choose i so that the scalar product is maximal. Geometrically one may think of the measurements as vectors and the scalar product will be large for vectors that point in the same direction.

It is also possible to use the second SVD basis function U_1^i and determine how well U^* can be represented by a linear combination of U_0^i and U_1^i.

This procedure may be viewed as a simple supervised learning algorithm where synthetic training data has been generated corresponding to simulations of measurements for various values of the physiological parameters. This data is then processed using the SVD algorithm which produces vectors $U_0^i, U_1^i, \ldots$, which are finally used to determine which location is most likely given an observed measurement U^*.

6.1 Singular Values

To verify that the singular values do indeed decay rapidly, Table 2 presents the first four singular values for the posterior ischemia and each perturbation

Table 2: *The singular values (sv) for the posterior ischemia, for the different perturbations performed on the ischemia.*

	sv 1	sv 2	sv 3	sv 4
translation	0.00169	0.0000471	0.00000598	0.000000733
changed lung cond.	0.00159	0.0000814	0.0000352	0.000000690
random cond.	0.00223	0.0000299	0.0000104	0.000000910
ischemia size	0.00131	0.0000250	0.00000355	0.000000442

As can be seen from the table, there is a rather large difference between the singular values. This same pattern was observed for each of the three remaining ischemia locations.

6.2 Perturbations

For each ischemia, the U_1-vectors from the different perturbations are shown. Red corresponds to the translation, green to the variations made to the size of the ischemic region, blue to the conductivity changes in the lungs and yellow is the random conductivities in the entire body. Figure 26 shows the perturbations for the anterior ischemia, Figure 27 for the posterior ischemia, Figure 28 for the inferior ischemia, and Figure 29 for the lateral ischemia.

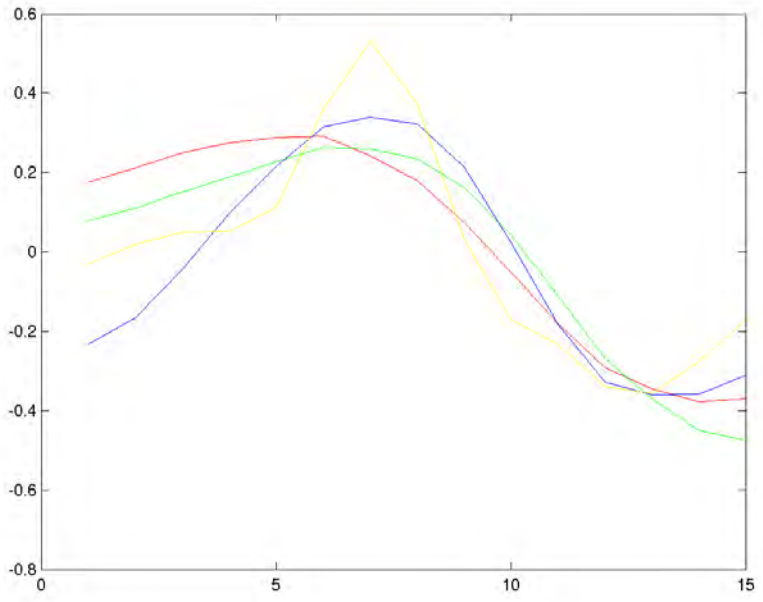

Figure 26: *The U_1 vectors for all the different perturbations for the anterior ischemia.*

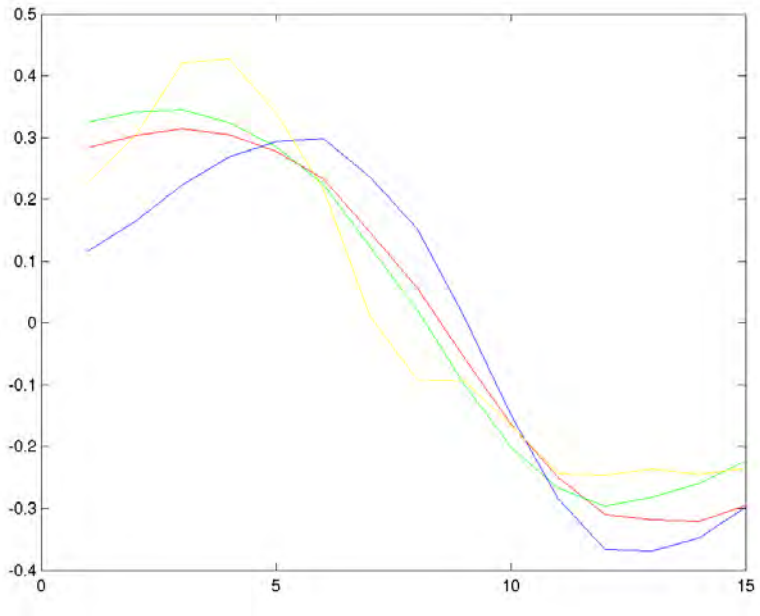

Figure 27: *The U_1 vectors for all the different perturbations for the posterior ischemia.*

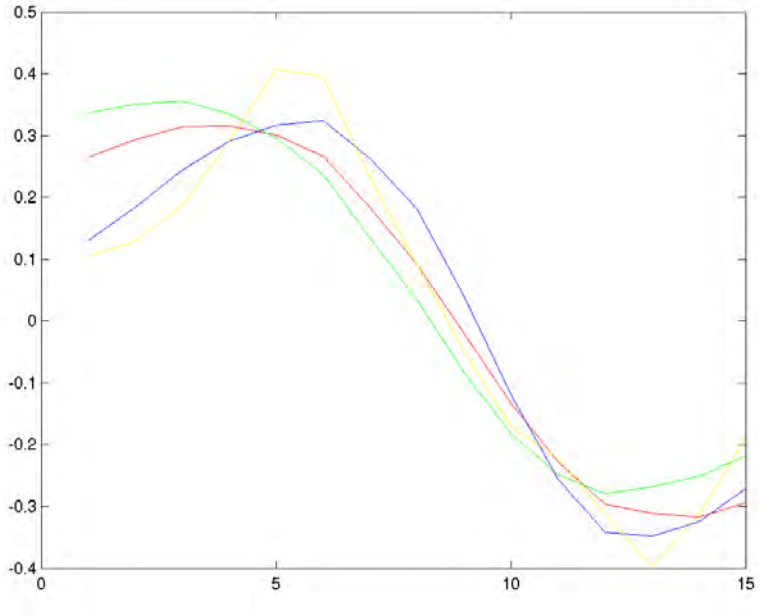

Figure 28: *The U_1 vectors taken for all the different perturbations for the inferior ischemia.*

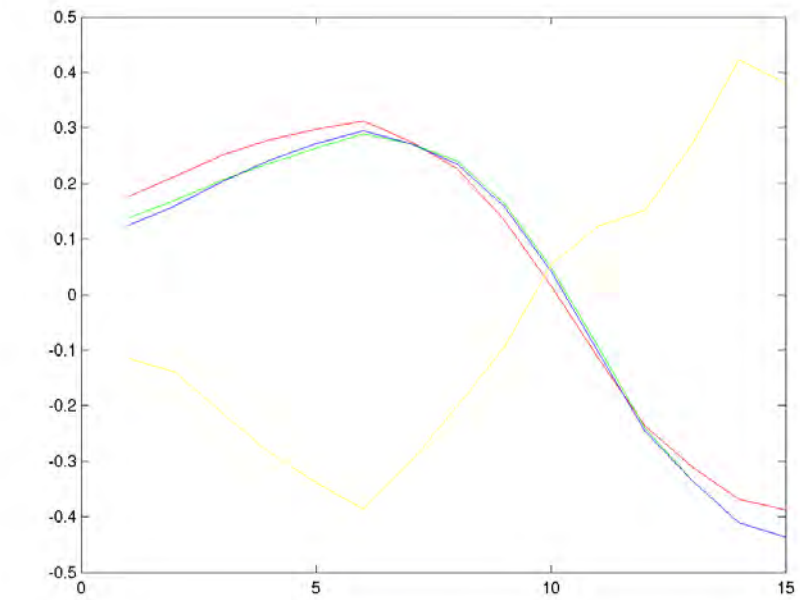

Figure 29: *The U_1 vectors taken for all the different perturbations for the lateral ischemia.*

6.3 Unknown Ischemia

To verify if it is possible to decide the location of an ischemia based on the results given from the different simulations, various random variations were made to the different physiological parameters for each ischemic location. The results can be seen in Figure 30 and the normalized results in Figure 31.

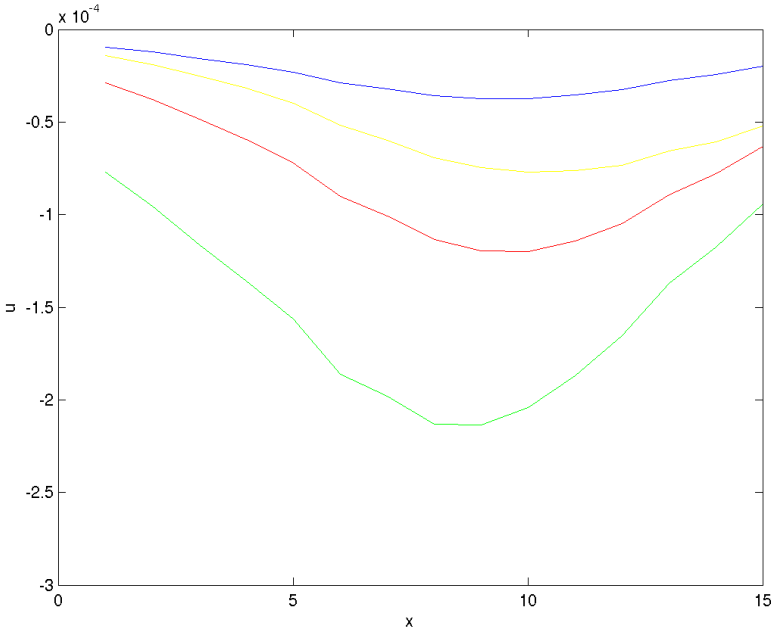

Figure 30: *Four unknown ischemia.*

For each ischemia, all the different perturbations were positioned into one large matrix and SVD was then performed on the matrix. To identify the "unknown" ischemia, the scalar product was taken between the U_0-vector of the matrix for each ischemia together with the vector from each "unknown" ischemia. The results of these scalar products can be seen in Table 3 below.

Table 3: *The scalar product between the four "unknown" ischemia and the U_0-vectors for each ischemia.*

	unknown 1	unknown 2	unknown 3	unknown 4
U_0^1	0.99999	0.99051	0.99990	0.99359
U_0^2	0.99164	0.99982	0.99312	0.97184
U_0^3	0.99871	0.99606	0.99923	0.98701
U_0^4	0.99337	0.96966	0.99218	0.99998

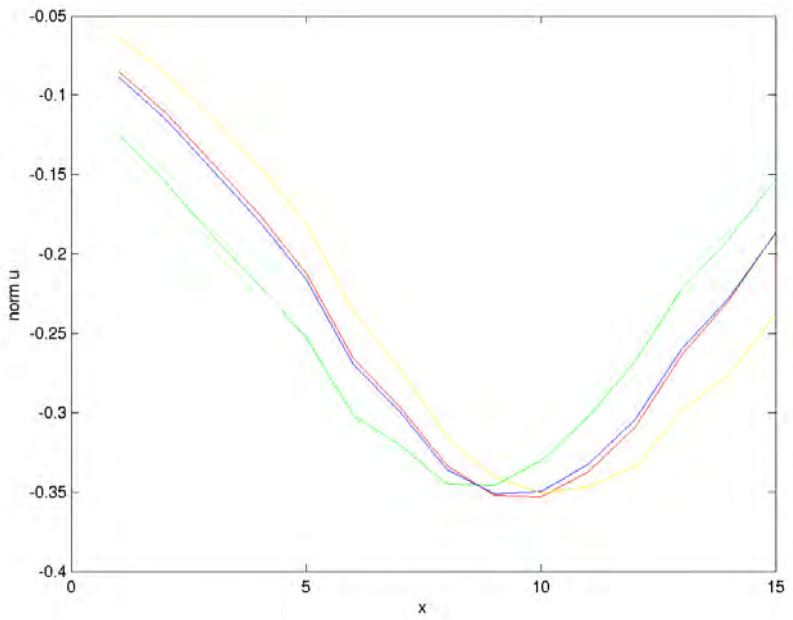

Figure 31: *Four unknown ischemia with normalized result.*

7 Discussion

The main question is *Is it possible to detect different types of ischemia based on ECG readings?* This thesis has come a way in trying to answer that question. Various physiological variations have been made to the mathematical model and the corresponding program and the results from these have been analyzed using the two methods of Singular Value Decomposition and Supervised Learning. In the following section, conclusions are made about the progress of the work and the results that have been obtained and in the final section the future work that could or perhaps should be done is discussed.

7.1 Conclusions

Restrictions

In the present thesis, the program that has been used to simulate the electrical activity of the heart has several restrictions. These restrictions can be separated into different parts. First of all, the model of the heart and the ischemic region is incomplete. As mentioned before, only the lower part of the heart is used and the fact that the heart conductivity is anisotropic is not taken care of. The spread of the ischemia is simulated as a sphere and the locations of the ischemia are based on a figure instead of real biological data. Throughout the report, the names given in Figure 3 have been used for the different ischemias. These names should perhaps more be seen as a way of separating the four different locations of the ischemias. The number of locations for the ischemias, is another restriction in this thesis. However, this is something that could easily be solved in contrast to some of the other restrictions.

Results

The results given in Section 5 and Section 6 are discussed below.

It was not possible to alter the location of the heart that much or the heart would have been outside the torso or embedded into the lungs. In Figure (10), it can be seen that the results for each ischemic region varies a little but comparing the variations for each ischemic region with each other, it is possible to distinguish each ischemia.

With increasing radius for the ischemic sphere, the values in the results also increases which is what could be expected. The normalized results are similar to the results from when the hearts location has been changed. It is possible to distinguish the ischemic regions from each other, except for some of the more extreme cases. The increasing values for each radius does not increase cubicly. An explanation to this could be the fact that when the ischemic sphere (as it is simulated) lies inside the heart wall the size of the sphere is proportional to the radius. However, when the sphere (radius) starts to become larger than the heart wall the ischemic region will no longer be a sphere, since the ischemic region only exists inside the heart wall. The size of the ischemic region will therefore not only depend on the radius of the sphere but also of the actual location it has in the heart and the geometry of the heart in surroundings of the ischemic region.

The chosen interval for the changed conductivity in the lungs is a lot larger than what could be expected in real life but it does give an idea of how the potential may vary with different lung conductivities. The results does not depend that

strongly on the varying conductivities in the lungs. Compare, for example, the 0.76 mS/cm with the 0.96 mS/cm, the difference is almost not noticeable. To get a significant change in the result, one has to look at conductivity values below 0.66 mS/cm or higher than 1.26 mS/cm. These values are probably not close to the real values of human lungs.

Changing the conductivity in the entire body using a random normal distribution with 5 % standard deviation it can be seen that it does not result in any larger changes in the results. The difference between the ischemic regions are large and they are well defined. Using the larger standard deviation, 10 %, the spread in the results are larger, especially for the anterior (red) and inferior (green) ischemia. But the normalized values are still relatively separated.

SVD are made to the different physiological variations. Since the singular values indicate a rank of approximately two for the matrix, only the first two U-vectors are used and the resulting U_1-vectors for each ischemia is shown in Figures 26 - 29. As can be seen, it can be quite tricky to separate the different vectors from each other, except for the random variations vector. This means that it might be difficult to find the size of the ischemic region since the vector obtained from that SVD is hard to separate from the hearts location vector and the lung conductivity vector. In Figure 29, the size and conductivity vector is almost equal. The fact that these two variations will be similar can be reasoned to. An increase in the ischemic region will correspond to a decrease in the lung conductivities.

Four unknown ischemic regions have been simulated and using the data obtained from all other simulations and doing SVD, it has been possible to distinguish each unknown ischemia using a scalar product between old values and the new, unknown ones. As mentioned in Section 6, this could be seen as a simple supervised learning algorithm. The SVD algorithm produces vectors $U_0^i, U_1^i, \ldots,$ which are used to distinguish each ischemia, as can be seen in Table 3. A large value is an indicator of how similar the two vectors are, and therefore what type of ischemia it is. As shown in Table 3, the scalar values differ and indicate that it is possible to determine an unknown ischemic region. However, for some scalar values, the difference for different ischemic regions are not very large. This could lead to problems in the identification process.

So, in conclusion, finding the correct size of the ischemia seems to be quite a difficult task. However, the location of the ischemia seems possible to find even when various physiological variations have been made to the model.

7.2 Future Work

As mentioned above, there are a number of restrictions made in this thesis. Several of these should be exploited in the future. The first and perhaps most obvious restriction is that it is only the stationary phase of the bidomain equations that are studied here. The time dependent equations are the next step. Coupled to this is the ionic models which are only briefly explained in Section 3.3.

As mentioned in Section 4.3.1 only the first part of three error contributions are included into the program. The other two have been included as this period of this thesis was nearing its end.

In this thesis, the solution has always been taken from a band on the torso. The

effect of where the solution is taken should be studied further, i.e. front and/or back of the torso, different heights in comparison to the heart and ischemia. Most likely, the region of choice will have a great impact on the possibilities of finding the correct ischemia based on the solution at the torso. In the present geometry used, there exists problems around the boundary of the torso due to the adaptivity, making it difficult to look exactly at the body surface. A better geometrical model is being worked on.

Something that will also affect the solution is the shape of the human figure. All of the results presented here are based on one persons figure which have been scanned using MRI. But, of course, the human body comes in all different shapes and sizes. Having generated a lot of data using one standard figure, a reference person, the idea would then be to scale every person and the corresponding results to this reference person. In that way, standardized results will be obtained which might then be used to determine the unknown ischemia location and size (using some optimization routine).

Another obvious restriction to this model is the fact that only the lower part of the heart is used, this is mentioned in Section 4.2 and the reasons as of today for doing this is explained. Nevertheless, in order to have a complete model of the electrical activity, the entire heart should be simulated. The conductivity in the heart is anisotrope due to the fiber structure. This is not taken into account in the present model and this feature should be included in the future.

Four regions of ischemia have been selected in this thesis. They are based on Figure 3. More biological data on the exact location of these should be used. Also, they are simulated as spheres, the real spread of an ischemia should be noted and more carefully simulated. Since only four locations (spheres) are used, the data achieved and the possibility of finding and classifying an unknown ischemia will be based on its closeness to one of the four locations. An idea is then to divide the entire heart into, say 20 locations (spheres) and generate data from these. This will extend the possibilities to find an unknown ischemia that could be placed in more places in the heart.

An alternative way of finding out what type of infarction a patient has by studying a given set of ECG recordings is called the inverse problem (or the parameter identification problem). This is well defined mathematically but, unfortunately, rather difficult to solve mathematically. There have been some material written on these subject and work is ongoing.

References

[1] Tortora G, Derrickson B *Principles of Anatomy and Physiology* 11th edition, Wiley & Sons

[2] Sundnes J, Lines G, Cai X, Nielsen B F, Mardal K-A, Tveito A *Computing the Electrical Activity in the Heart.* Simula Research Laboratory, 2005.

[3] Golub G H, Van Loan C F *Matrix computations.* 3rd Edition, Johns Hopkins University Press, Baltimore, Maryland, 1996.

[4] Lau J, Ionnadis P, Balk E M, Milch C, Terrin N, Chew P W, Salem D *Diagnosing acute cardiac ischemia in the emergency department: a systematic review of the accuracy and clinical effect of current technologies.* Ann. Emerg. Med., 37 (2001), pp.453-460.

[5] Birnbaum Y, Drew B J *The electrocardiogram in st elevation acute myocardial infarction: correlation with coronary anatomy and prognosis.* Postgrad. Med. J., 79 (2003).

[6] Tung L *A bi-domain model for the describing ischemic myocardial D-C potentials.* PhD thesis, MIT, Cambridge, 1978.

[7] Internet webpage, 2006, http://en.wikipedia.org/wiki/Heart

[8] Nielsen B F, Lysaker M, Tveito A *On the use of the resting potential and level set methods for identifying ischemic heart disease; an inverse problem* Nov 11 2005

[9] MacLachlan M C, Sundnes J, Lines G T *Simulation of ST Segment Changes During Subendocardial Ischemia Using a Realistic 3-D Cardiac Geometry.*IEEE Transactions on Biomedical Engineering, Vol. 52, No. 5, May 2005

[10] Internet webpage, 2006, http://mathworld.wolfram.com/Box-MullerTransformation.html